Biophysical Chemistry 148 (2010) 74–81

Contents lists available at ScienceDirect

Biophysical Chemistry

journal homepage: http://www.elsevier.com/locate/biophyschem

The role of asymmetric binding in ligand–receptor systems with 1:2 interaction ratio

David G. Míguez *

Department of Systems Biology, Harvard Medical School, Boston, MA 02115, USA

ARTICLE INFO

Article history:
Received 27 December 2009
Received in revised form 5 February 2010
Accepted 19 February 2010
Available online 25 February 2010

Keywords:
Ligand–receptor systems
Erythropoietin
Asymmetric binding
Stochastic modeling

ABSTRACT

Dynamical models for cellular ligand–receptor systems are among the most successful examples of mathematical approaches in systems biology. Here we present a general kinetic and mechanistic model for systems with asymmetric 1:2 ligand–receptor interaction ratio, such as erythropoietin and growth hormone systems. In these systems, the ligand presents two very different binding affinities to its receptor, and the weak interaction being often neglected for modeling purposes. Here, we demonstrate that the weak binding is the one tightly regulating the signaling, while the strong binding sets the threshold for the auto-inhibition effect characteristic of 1:2 asymmetric ligand–receptor systems. The model constitutes an improved mathematical framework for erythropoietin activation and equivalent biological processes, which are, due to their widespread use and relevance, on the forefront of pharmacological systems biology.

1. Introduction

Cell-surface receptors are the primary means by which cells detect external stimuli and environmental changes, and they enable cell communication in higher organisms. They are also among the most well established therapeutic targets for treatment of diverse illnesses, including cancer, AIDS and anemia [1–4,6]. Receptors are activated by ligands, including cytokines, hormones and growth factors, leading to a downstream cascade of posttranslational modification events eventually regulating cell fate [7]. Mathematical models that combine extracellular (ligand–receptor binding, diffusion) and intercellular processes (regulation, endocytosis, recycling and degradation) have been recently proposed for ligand–receptor systems interacting in a 1:1 ratio [8–10].

Quite commonly, ligands and receptors interact in a 1:2 ratio, with the ligand interacting with two identical receptors via two different binding sites. Among the most studied systems showing a 1:2 interaction scheme stands erythropoietin (EPO), a glycoprotein hormone required for mature red blood cell production with anti-apoptotic properties [11]. In the same group of the cytokine receptor superfamily and sharing the same activation mechanism is growth hormone (GH). GH is the key regulator of postnatal growth, playing a very important role also in metabolism, and in the reproductive, gastrointestinal, cardiovascular, hepto-biliary and renal systems [12]. Interestingly, the two binding sites present in each EPO and GH ligand have dramatically different affinity towards its receptor (up to three orders of magnitude) [13], and models for such systems commonly neglect the weak binding and assume a 1:1 ligand–receptor dynamics governed by the strong interaction [14].

In this paper, we present a general mathematical model for systems following the same interaction scheme as EPO and GH, accounting for 1:2 interaction ratio and the ligand presenting asymmetric binding affinity for each of the receptor of the complex. The model allows us to unveil the implications of such particular interaction scheme and the role of each ligand binding site in the mechanism. In particular, the model shows that, for asymmetric 1:2 interaction, the weak binding site is the one in charge of the tight regulation of the amount of complex formation and, in consequence, the signaling. We also study the role of each binding site in other characteristic situations of these systems, as the effect of ligand homodimers and the auto-inhibition observed at high ligand concentrations.

In addition to the ligand–receptors interactions occurring in the cell surface, the model incorporates the main regulatory processes in receptor production and trafficking. As a numerical solution, we use parameter values of the EPO system (see Table 1). The model is also valid for GH and variants of EPOR and EPO molecule, (including the increasingly important NESP molecule [15]), or even other ligand–receptor systems with asymmetric binding properties.

2. Models

The model is composed of six species, each representing a different configuration of the ligand–receptor complex (Fig. 1). The species are involved in the following four reversible and five irreversible interactions:

$$R + L \underset{k_{1.off}}{\overset{k_{on}}{\rightleftharpoons}} C_1 \tag{1}$$

* Present address: Instituto de Biologia Molecular de Barcelona, CSIC, Parc Cientific de Barcelona, C/Baldiri i Reixac 15-21 Barcelona 08028.
E-mail address: dgmbmc@ibmb.csic.es.

0301-4622/$ – see front matter © 2010 Elsevier B.V. All rights reserved.
doi:10.1016/j.bpc.2010.02.012

Table 1
Kinetic, physical and structural parameters for EPO.

Parameter	Value	Reference and notes
R_T	1000 molec./cell	Ref. [20,21]
$k_{1,off}$	29 min^{-1}	Ref. [14]
k_{on}	0.029 min^{-1} nM^{-1}	Ref. [14]
$K_{1,D}$	920 nM	Ref. [13]
$k_{2,off}$	0.029 min^{-1}	Ref. [13]
$K_{2,D}$	1 nM	Ref. [13]
$k_{3,in}$	0.06 min^{-1}	Ref. [14]
$Q_{R,0}$	10 nM min^{-1}	Ref. [20,21]
k_{rec}	0.036 min^{-1}	Ref. [14]
k_{deg}	0.024 min^{-1}	Ref. [14]
$k_{R,in}$	0.01 min^{-1}	Ref. [8]
V	4×10^{-10} L/cell	Ref. [8]
L_0	0.2 nM	Ref. [13]
r	8.5 μm	for Hela cells. Ref. [39]
D	0.084 $\mu m^2/s$	Ref. [40]
h	7.27×10^{-3} μm	Ref. [41]
a	3×10^{-3} μm	Ref. [41]

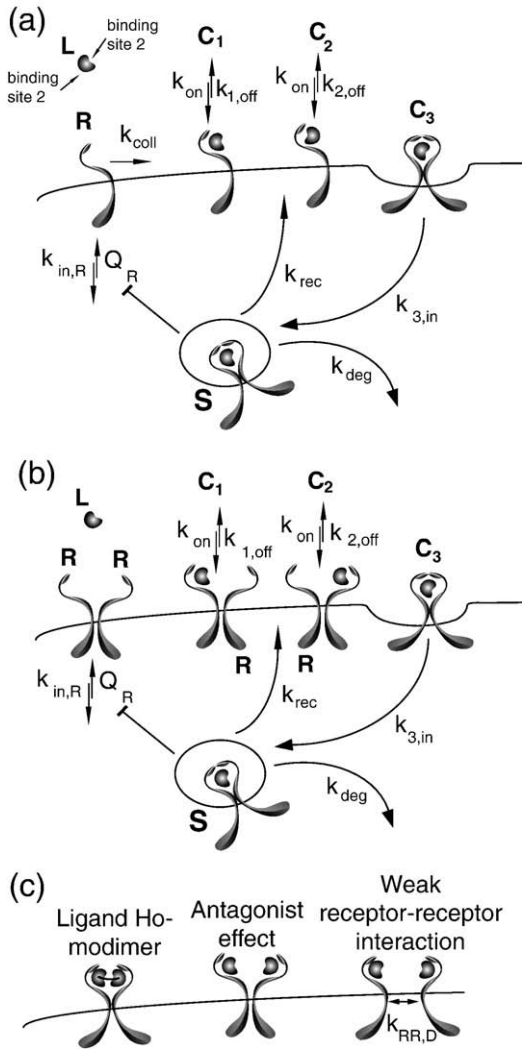

Fig. 1. Scheme for the model components and their kinetic parameters. Illustration of the kinetic values and their significance for the (a) receptor monomer model and (b) receptor dimer model; (c) illustration of the active complex formation during auto-inhibition and homodimer ligand stimulation in the receptor dimer model and the model for weak interaction of receptors.

$$R + L \underset{k_{2,off}}{\overset{k_{on}}{\rightleftharpoons}} C_2 \tag{2}$$

$$C_2 + R \underset{k_{1,off}}{\overset{k'_{on}}{\rightleftharpoons}} C_3 \tag{3}$$

$$C_1 + R \underset{k_{2,off}}{\overset{k'_{on}}{\rightleftharpoons}} C_3 \tag{4}$$

$$C_3 \xrightarrow{k_{3,in}} S \tag{5}$$

$$S \xrightarrow{k_{rec}} L + 2R \tag{6}$$

$$S \xrightarrow{k_{deg}} \nexists \tag{7}$$

$$\nexists \xrightarrow{Q_R} R \tag{8}$$

$$R, C_2, C_1 \xrightarrow{k_{R,in}} \nexists \tag{9}$$

Eqs. (1) and (2) represent the two possible reactions in which a free ligand (L) first associates with a free receptor molecule (R) to produce the intermediate complexes C_1 and C_2. The subscripts indicate the two different possibilities for the binding of the ligand with the receptor, depending on which one of the binding sites of the ligand is used in the formation of the intermediate complex. C_3 represents the active complex and S is the active complex internalized by endocytosis . In these type of systems, the affinity rate constant k_{on} is commonly assumed to be the same for both reactions, since this value is mainly dependent on structural and rotational aspects [7]. On the contrary, the two binding sites can have different dissociation rate constants, $k_{1,off}$ and $k_{2,off}$. The affinity and dissociation rate constants are related by the dissociation constant $K_{1,D} = k_{1,off}/k_{on}$ and $K_{2,D} = k_{2,off}/k_{on}$.

Eqs. (3) and (4) represent the second binding reaction of a free receptor (R) with the intermediate complexes C_1 and C_2. Formation of the active complex C_3 can only occur through the available binding siteof the ligand inside the intermediate complexes C_1 and C_2, i.e., C_2 can bind to R only via the free $K_{1,D}$ (Eq. (3)), while C_1 can bind to R only through the free $K_{2,D}$ in the ligand (Eq. (4)). For dimensional consistency, the total number of complexes formed through reactions 1 and 2 is rewritten as a concentration value:

$$L_1 = \frac{C_2}{N_{Av}V_0} = \frac{3C_2}{4\pi N_{Av}}\frac{1}{(r+h)^3 - r^3} \tag{10}$$

$$L_2 = \frac{C_1}{N_{Av}V_0} = \frac{3C_1}{4\pi N_{Av}}\frac{1}{(r+h)^3 - r^3} \tag{11}$$

where N_{Av} is the Avogadro's number, V_0 is assumed to be a spherical gasket with height equal to the extracellular height of the receptor–ligand complex h, and inner radius equal to the average cell radius r.

Regarding the configuration of the unstimulated receptors in the membrane, we will test the receptor diffusing as monomers (Fig. 1a) or as dimers prior to ligand stimulation (Fig. 1b) [34]. The model will be initially developed for freely diffusing receptors R and intermediate complexes C_2 and C_1. The model for receptor dimers and their implications will be discussed in Appendix A. For the case of receptor diffusing as monomers, the formation of the complex will be modulated by the diffusion constant D and the collision rate constant k_{coll} of receptors R intermediate complexes C_2 and C_1, and, the characteristic affinity rate constant k'_{on} is modulated in the following way [7]:

$$k'_{on} = \left(\frac{1}{k_{on}} + \frac{1}{k_{coll}}\right)^{-1} = \left(\frac{1}{k_{on}} + \frac{ln(b/a)}{2\pi DhN_{Av}}\right)^{-1} \tag{12}$$

Parameter D corresponds to the diffusion coefficient of the receptor, and a is its width. Parameter b is the average distance between free receptors R in the cell, calculated assuming a homogeneous distribution of receptors on a cell surface of radius r as follows:

$$b = \sqrt{\frac{4r^2}{R}} \tag{13}$$

Since the number of free receptors R diminishes after ligand stimulation, the collision rate constant k_{coll} and therefore the affinity rate constant k'_{on} are time-dependent variables. Recent experiments highlighted the importance of an appropriate orientation in the activation of the receptor complex [16], which may further reduce the effective collision rate constant (k_{coll}) obtained from Eq. (12), increasing the effect of diffusion. Our model does not account for these corrections in k_{coll}.

Since the ratio between k_{coll} and the affinity rate constant k_{on} depends on R, the mechanism of active complex formation can change from being a reaction-limited ($k_{coll}>>k_{on}$) to a diffusion-limited ($k_{coll}<<k_{on}$) process along the experiment.

Reactions 5 through 9 account for endocytosis and trafficking of the active complex into the cell [8]. Specifically, reaction 5 accounts for the internalization of the active complex S, with internalization rate constant $k_{3,in}$. Reaction 6 accounts for the recycling of S with a rate constant of k_{rec}. The parameter k_{deg} and Q_R in reactions 7 and 8 correspond to the degradation rates of internalized complexes and production of fresh receptor R, respectively. Degradation is represented here by the mathematical symbol ∄. Finally, reaction 9 corresponds to the internalization and constant degradation of the unstimulated receptors and the intermediate complexes R, C_2 and C_1. The dynamic equilibrium that keeps a constant concentration of receptors in absence of ligand stimulation ($L=0$) depends on the balance between reactions 8 and 9.

Numerical values for the simulations corresponding to the EPO ligand–receptor system were obtained from the literature and are listed in Table 1. Parameters and products corresponding to an interaction through the weak binding site of the ligand are labeled with the subindex 1 (reactions 1 and 3), while the strong binding reaction is labeled with the subindex 2 (reactions 2 and 4).

The parameter $k_{R,in}$ is assumed to be six times smaller than the parameter $k_{3,in}$, mimicking the known ratio of internalization rates for free receptors and complexes in similar systems [8].

For the EPO system, free receptor production Q_R have been shown to be down-regulated after ligand stimulation [17,18]. We introduced this dependence in the form of a Hill function of the internalized complex S, with n representing the cooperativity [19]:

$$Q_R = Q_{R,0}\left(1-\frac{S^n}{S^n+\theta^n}\right) \tag{14}$$

We assumed cooperativity $n=2$ and threshold $\theta=1$ as appropriate values for repression systems. Higher cooperativity and lower threshold numbers produce stronger down-regulation, slightly reducing the time for the system to reach steady state after stimulation. We set the value $Q_{R,0}$ to maintain the constant amount of receptor R_T reported [20,21] in absence of ligand. We did not consider non-specific interactions of the ligand with other receptors present on the cell surface, nor we did consider receptor orientation and clustering [7].

Importantly, the low number of molecules involved in these processes does not allow for a deterministic numerical integration scheme, and stochastic integrations of the model are more accurate in their predictions. In the case of EPO, the number of total receptors R_T is low enough to require an stochastic integration scheme, so we implemented the well-known Gillespie algorithm [22–24] as the most widely used method for stochastic modeling. The deterministic version of the model, valid for systems involving higher number of molecules, is also presented and discussed in the Appendix B.

Simulations and data analysis were performed using Matlab 7 (The Mathworks, Natick MA) using programs developed in-house. Numerical computations were run on a desktop computer. Code is available upon request. Total time frame for the simulations is 300 min, so no corrections due to cell growth cell division (around 20 h for a T-cell) are taken into account [5].

3. Results

3.1. Intermediate complex formation increases locally the ligand concentration and favors the weak binding

Numerical integration of the model using the parameters listed in Table 1 is shown in Fig. 2. Fig. 2a corresponds to the receptor monomer model. Fig. 2b corresponds to the receptor dimer model (explained in Appendix A). After ligand stimulation at time t = 0 min, there is an increase of the intermediate C_2 strong complex (dash gray line), with a peak at t = 40 min, followed by a relaxation to a steady state at $t=200$ min. The amount of the weak complex C_1 (dash black

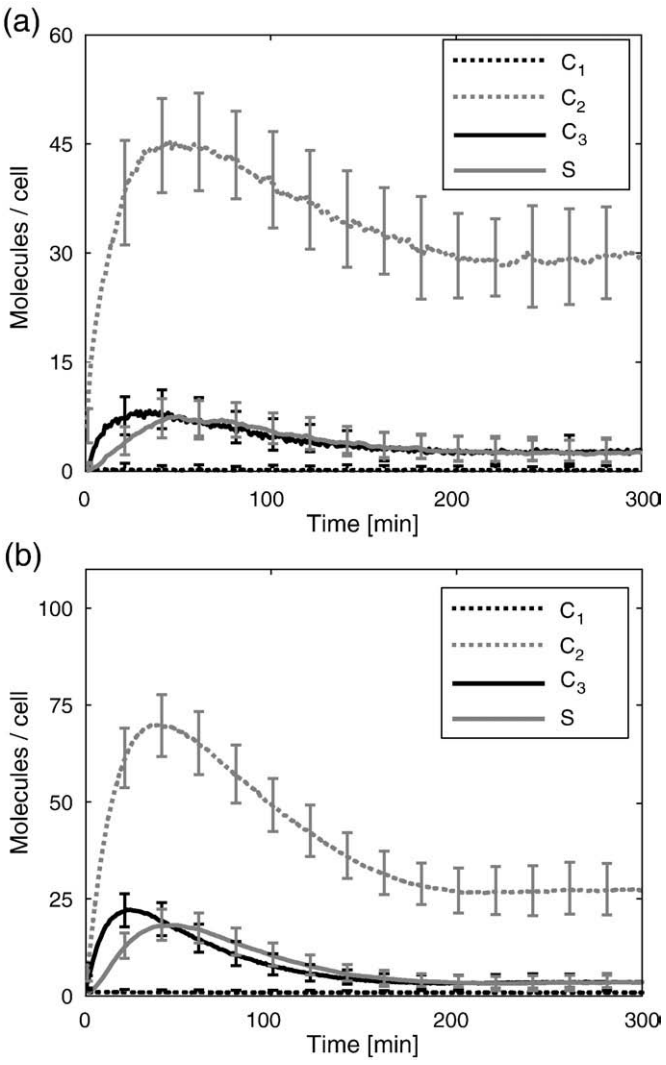

Fig. 2. Dynamics of the different model variables after ligand stimulation. Numerical integration for the (a) receptor monomer and (b) receptor dimer model (see Appendix B). Bars represent the standard deviation calculated for 100 numerical integrations of the stochastic algorithm.

line) remains steady at values close to zero at all times. The profiles of the active C_3 and internalized S complexes follow a similar temporal profile than C_2.

For the ligand concentrations used here, only a maximum of 4.5% (Fig. 2) of the initial total receptors R_T are bound to ligand via the strong binding site (C_2), while almost none receptors (an average of less than 0.1%) are bound via the weak site (C_1) (10 C_3 molecules at time $t = 20$ min). Since this weak binding is necessary for the active complex formation C_3, to understand why complexes are being formed despite the weak interaction $k_{1,off}$ of this key reaction (around 1000 times weaker than the strong binding $k_{2,off}$), we computed the local concentration of the ligand at the cell surface, created by the intermediate complexes.

Fig. 3 is a plot of the temporal evolution of the local ligand concentration in its three possible forms: L_2 is the ligand with a free weak binding site (black line), L_1 is the ligand with a free strong binding site (gray line) and L correspondsto the free ligand (dashed line). After stimulation, the model predicts an increase in L_2 to a steady value two orders of magnitude higher than the free ligand concentration L. This way, the weak binding reaction and the formation of C_3 complex takes place due to a local concentration increase of ligand with free weak binding site close to the cell surface, which favors the weak reaction 3. On the other hand, the small amount of intermediate complexes formed only throughthe weak binding site C_1 (reaction 1) quickly interacts with free receptors through the available strong binding site (reaction 4), reducing even more the amount of this intermediate complex in the cell surface. Theligand concentration L is in excess and therefore remains almost constant during the process (dashed line).

3.2. Active complex formation is regulated by the weak binding

We analyzed the dependence of each binding site on the regulation of receptor–ligand–receptor complex formation C_3 by performing simulations for different values of the two dissociation constants for the ligand (see Fig. 4. Fig. 4a was calculated by fixing the dissociation constant for the weak binding $K_{1,D}$ while varying the dissociation constant for the strong binding $K_{2,D}$ two orders of magnitude. In Fig. 4b, we varied $K_{1,D}$ while $K_{2,D}$ was fixed. The vertical dash–dot line in each figure correspond to the wild type value, labeled as $K^{WT}_{1,D}$ and $K^{WT}_{2,D}$.

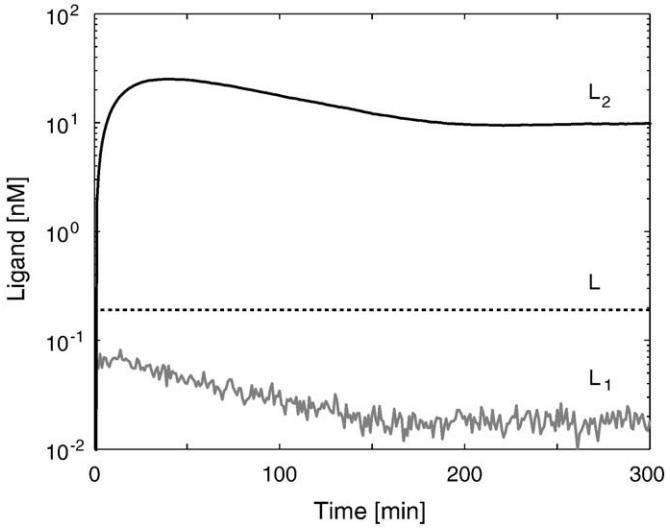

Fig. 3. Strong binding creates a local concentration increase that favors the weak binding interaction. Numerical integration for the local concentrations of ligand in the different conformations (L = free, L_1 = ligand with free strong binding site, L_2 = ligand with free weak binding site) on the cell surface.

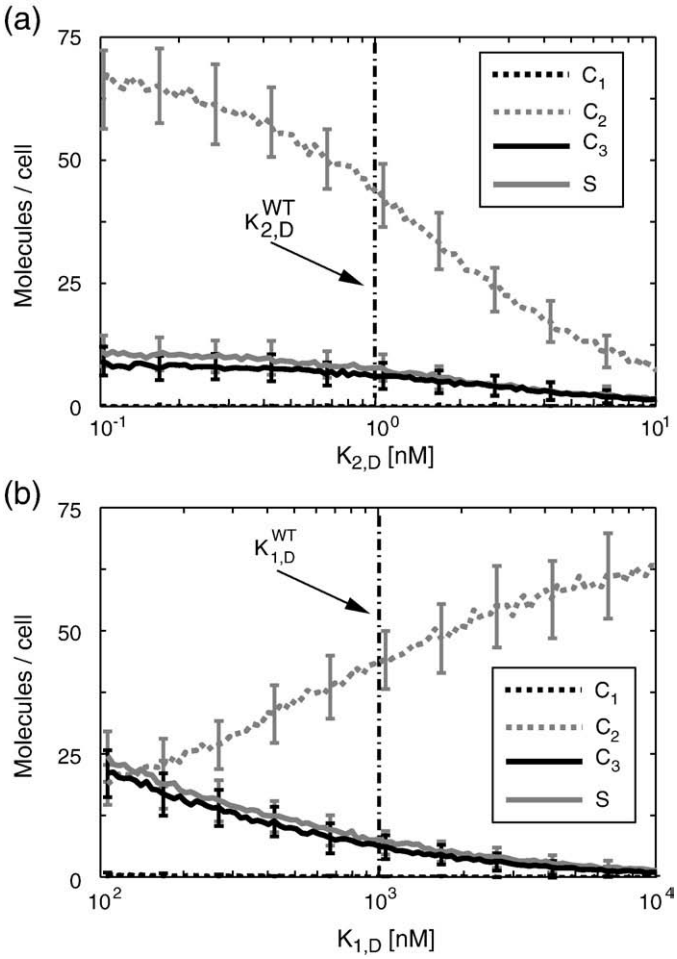

Fig. 4. The weak binding interaction regulates the total amount of active complex. Dependence of complex formation for the (a) dissociation constant for the strong binding interaction and (b) dissociation constant for the weak binding interaction at time $t = 40$ min. Bars correspond to the standard deviation calculated for 100 numerical integrations of the model.

Changes in the strong binding site (Fig. 4a) producing a 6-fold change in the active C_3 (solid black line). On the contrary, the same variation on the weak binding site (Fig. 4b) produces a 20-fold change in the amount of active complex C_3 (solid black line) evidencing that the weak binding site is a stronger regulator of active C_3 formation that the strong binding site.

Interestingly, the strength on the weak binding also strongly regulates the amount of ligand–receptor linked via the strong binding C_2, but in a inverse fashion as the strong binding. Decreasing $K_{2,D}$ increases C_2 (Fig. 4a, gray dashed line), while decreasing the weak $K_{1,D}$ decreases the amount of strong binding complex C_2 (Fig. 4b, gray dashed line) to the expenses of the formation of the active C_3. This dependence shows that the weak binding reaction is indeed the limiting step for C_3 formation, showing why this weak interaction is the main regulator in the formation active receptor–ligand–receptor complex.

3.3. Homodimer shows increased activity relative to monomer due to specular structural characteristics

When the weak binding site in the ligand is replaced by a strong binding, the change in the levels of the receptor stimulation evidences the sensitivity of the system in the regulation by the weak binding site. This has been experimentally observed *in vivo* and *in vitro* by measuring cellular stimulation with homodimer molecules of GH–GH

and EPO–EPO ligands. These molecules have been shown to successfully drive formation of functional complexes and signal activation, showing remarkably enhanced activity compared to their monomers [25–28].

We have tested the effect of ligand homodimers by performing simulations assuming now that active C_3 complexes can be formed by interaction with the two strong binding sites of the ligand homodimer. In this configuration, the weak binding sites in the ligand are not longer necessary for complex activation and can be neglected. The results are plotted in Fig. 5.

The model shows a six fold increase in the maximum active complex C_3 (black solid line) and internalized S (gray solid line), when compared to the monomer molecule. This result is in agreement with experimental observations using homodimer molecules [25,26], and in agreement with the hypothesis that the existence of two strong bonding sites per molecule greatly contributes to the measured increase in activity for the homodimers with respect to the corresponding monomers [27,28].

The total amount of intermediate complexes (dashed lines) C_1 and C_2 (which are equivalent in this configuration) is lower than the ligand-monomer case (Fig. 2 a). This evidences that as soon as an intermediate complex is formed it interacts with a free receptor and forms a C_3 complex. From here, it follows that, for the ligand-monomer case, intermediate complexes are present in the system mainly due to theweak binding $K_{1,D}$, again reinforcing the importance of this weak binding in the mechanism.

3.4. Self-antagonist effect is regulated by the strong binding site

We also studied the role of each binding site played on the auto-inhibitory mechanism characteristic of these systems at high ligand concentrations. This auto-inhibition occurs due to a reduction in the number of free receptors R, eventually leading to a situation where most the receptors are bound to a ligand in an inactive C_1 or C_2 state, inhibiting the formation of C_3. This mechanism, known also as "self-antagonist effect", has been reported experimentally for EPO and GH systems [29,30].

We performed simulations to compute the amount of active complex C_3 formed depending on the ligand concentration L for different values of the dissociation constants. Results are plotted in Fig. 6, where the black solid line corresponds to wild type values of $K_{1,D}$ and $K_{2,D}$. The gray solid lines corresponds to different dissociation constants for the weak binding interaction $K_{1,D}$ and dashed gray lines correspond to different dissociation constants for the strong binding interaction $K_{2,D}$. The ligand concentration L is varied up to two orders of magnitude of the previously used value [13].

Focusing first on the wild type profile (black solid line), the number of C_3 has a peak at $L = 3$nM and then decays due to the auto-inhibition, with a maximum of $C_3 = 14$. When the weak binding site is varied (gray solid line), the maximum of C_3 gets dramatically increased, and the location of the maxima gets slightly shifted towards higher L values. It can be still observed a reduction at high L due to the auto-inhibition (negative slope regimes in gray lines). On the contrary, when the strength of the strong binding $K_{2,D}$ is increased, the maximum in C_3 increases slightly, but the auto-inhibition effect is not observed for these values of L, with C_3 always increasing when L is increased.

4. Discussion

The model here presented allows us to unveil the distinct roles that each of the binding sites on the ligand is playing in the process of C_3 formation. The strong binding is necessary to increase the local concentration of ligand on the cell surface to favor the interaction with the receptor through the weak binding site (reaction 3). The fact that such a weak interaction occurs at relevant experimental times cannot be explained only by the high concentration of C_2, and the effect of the local concentration increase of ligand close to the cell surface (shown in Fig. 3) is the key. In absence of this local concentration increase and with the ligand concentrations commonly used in experiments [13], weak binding interaction and, therefore, active complex formation will occur on a time scale of days.

Surprisingly, the role of regulating the amount of signaling complex on the cell surface appears to be played by the commonly neglected weak binding interaction [14]. Only when the affinity of the weak interaction is modified, the total amount of active C_3 complexes changes significantly, as shown in Fig. 4 and in Fig. 6.

This regulatory role is also reflected when ligand homodimers are used, where presumably the weak binding is not necessary for C_3

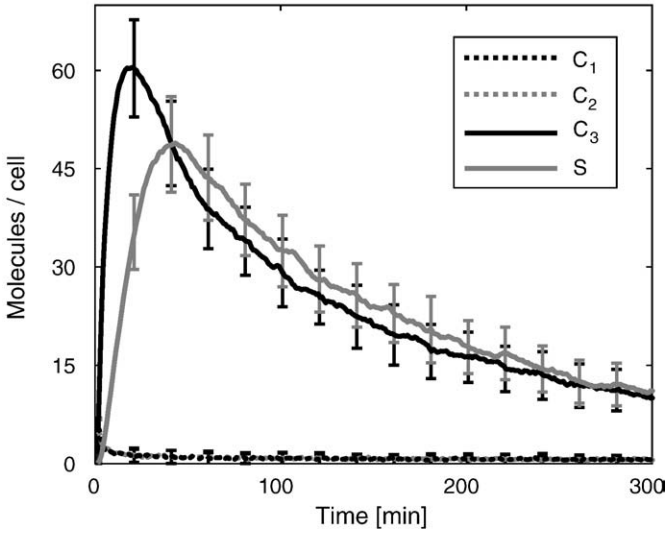

Fig. 5. Ligand homodimer shows increased activity due to the two available strong binding sites. Numerical integration for the stochastic model for the homodimer case. Bars represent the standard deviation for 100 numerical integrations of the stochastic algorithm.

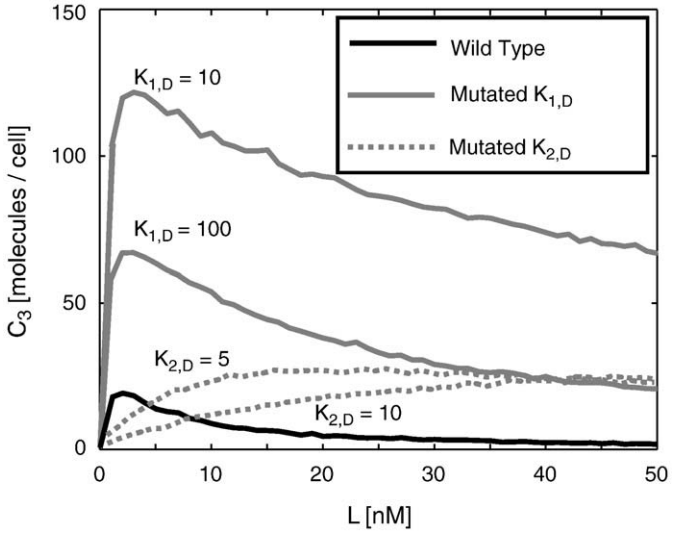

Fig. 6. Auto-inhibition effect is determined by the high affinity binding. Dependence on C_3 on the ligand concentration for various values of the two different dissociation constants at time $t = 40$ min. Each line corresponds to 50 computations of the model (each one averaged over 100 simulations). Bars for standard deviation are not plotted for clarity.

formation. In this case, the regulation of the weak site is lost and the signal gets increased compared with the ligand-monomer case, in agreement with experimental data. In addition of driving the local concentration increase, the strong binding site in the ligand appears also to be the main regulator for the self-antagonist effect. Changes in the strenght of the strong binding site of the ligand dramatically influences the behavior of the system at high ligand concentrations, and the optimal ligand for maximum activity is very much dependent on the affinity of this strong site. Since the auto-inhibition acts as a "mechanistic" signal regulation in response to elevated doses of ligand, the strong binding sets up the optimal ligand value for maximal activity before auto-inhibition takes place and reduces signal strength.

The fact that these type of systems with 2:1 asymmetric interaction present such different affinities (1000 fold difference) provides them with their very specific characteristics, as the auto-inhibition and the tight regulation via a a very low affinity binding interaction. The results here shown predict that mutation experiments to modify the activity of the ligand will be more effective when performed in its weak binding site. On the other hand, mutations on the strong binding site will reduce auto-inhibition and will allow for better tolerance to higher ligand concentrations without increasing ligand activity.

One of the simplifications of the present mathematical model is the assumption of a simple interaction scheme in the form of a Hill function to account for the down-regulation of production after ligand stimulation (reported in [17,18]). This mechanism most likely occurs via transcription factor repression of the promoters that control the transcription of the receptor gene. Most of the main details and parameters of this interaction are not known, but it will probably be more complex than a Hill function, with longer time scale interactions due to transcription/translation delay, and inherent noise due to genetic interactions [32]. Exploration of the parameters of this interaction (cooperativity n and threshold θ) does not significantly changes the result of the numerical computations and do not interfere with the main conclusions regarding 2:1 ligand–receptor interaction. Therefore, receptor down-regulation has been simplified to a Hill function to not undermine the main focus of the paper.

Another of the main assumptions of the model is related to some parameters of the two possible ligand–receptor interaction. It is possible that the ligands experience a conformational change after the first binding event, so the K_D's of the ligands will be different before and after this first interaction. According to crystalographic measurements [31], the NMR structures of a derivative of EPO called MLKysEPO, (EPO has low solubility and stability) shows very high similarity between the soluble form and the receptor bounded form of the ligand. A slight shift has been observed in the area close to the binding site that can potentially influence its binding affinity, but it is also highly probable that this small conformational change may be directly due to ligand being inside the two-receptor complex, and not just a consequence of the first binding. Therefore we assumed identical K_D's before and after binding. In addition, the weak binding dissociation constant $K_{1,D}$, (which we show as the one regulating the active complex formation) has been measured in conditions where the binding to the first stronger site has already occurred (see Ref. [13]). Since the K_D's are measured in solution, the effect of two dimensional diffusions of the receptors in the membrane needs to be introduced for the second interaction. This is also commonly introduced through a simple modulation in k_{on} via Eq. (14).

Another potential limitation of the model is that we have assumed the difference between the two binding events resides on the k_{off}, since the k_{on} is often assumed to depend only on structural and rotational aspects of the ligand [7]. To ensure that this assumption does not compromise the model predictions, the other situations need to be analyzed. The situation where the affinity of the weak site is greater than the strong binding ($k_{1,on}>k_{2,on}$) will actually favor the effect of the local concentration (C_2 is multiplying k_{on} in the equations). If, on the other hand, we assume that $k_{1,on}<k_{2,on}$, the effect of the local concentration will be indeed reduced, and the amount of active complex formed will be reduced accordingly. Lower $k_{1,on}$ implies lower $k_{1,off}$ (to maintain the value K_1, D measured experimentally), and this will result in less complexes being formed but more stably. Against this argument, SEC experiments with light scattering detection [13] have shown that the weak binding is much more easily dissociated (i.e., much less stable) than the strong binding.

Regarding other possible enhancements in the interaction scheme, no corrections on the rotation or proper orientation of the receptor/ligand complex have been introduced. This probably will increase the fitting of the experimental data at the expense of a more complex model, with a higher number of interactions and parameters to determine.

5. Conclusions

We developed a stochastic mathematical model for asymmetric 1:2 ligand–receptor systems that include ligand–receptor interaction, receptor diffusion, regulation, endocytosys, recycling and degradation. We have shown that the two binding sites play a distinct role in complex activation: the strong binding creates a local concentration of ligand on the cell surface that facilitates the weak binding. On the other hand, the weak binding (commonly neglected in models for these type of systems), tightly regulates the formation of the active complex, and therefore, the signaling. We have also shown that ligand homodimers exhibit increased activity due to the loss of the regulation via the weak binding. Finally, the auto-inhibition effect creates an optimal ligand concentration which only depends on the strength of the strong binding site. We conclude that both binding sites in the ligand play a very important and distinct role in the active complex formation, and none of them can be neglected without losing key aspects of the regulation.

In summary, our model provides a tool to understand in greater qualitative and quantitative detail the whole mechanism and the underlying complex regulation of ligand–receptor systems with interaction in a 1:2 ratio. The importance and the widely spread pharmacological use of EPO is itself a strong rationale for more accurate models to complement the recent increasing experimental efforts in endocrinology. The model results can be also applied to systems sharing a similar mechanism, as GH and NEST. Detailed ligand–receptor models help to understand the interaction between cells and their environment by providing a better interpretation of experimental biological data.

Acknowledgments

DGM acknowledges the financial support from the Ministerio of Educación y Ciencia of Spain for a postdoctoral fellowship and the European Commission for a Marie Curie International Reintegration Grant. Thanks to Pablo Cironi, Suzzane Komili, Dale Muzzey, Laura Sontag, William W. Chen, Michael M. Menzinger and Julie K. Gound, for useful comments and detailed reading of the manuscript.

Appendix A. Receptor monomer versus receptor dimer hypothesis

It has been recently proposed that free receptors may exist in a dimer configuration prior to ligand stimulation [12,33,34]. The classical model accepted for EPO and GH suggests that intermediate complexes (C_2 or C_1) and the free receptors R exist as monomers diffusing on the cell surface, with the ligand driving receptor dimerization [35–38]. In this situation, the reaction between (C_2 or C_1) and the free receptors R is modulated by the collision rate of receptors in the cell membrane (see Fig. 1a). A scheme for this model can be found in Fig. 1a.

On the contrary, recent experimental data suggest that EPO receptors exist in a pre-dimer configuration and the ligand only induces a conformational change in the receptor homodimer complex [33] that propitiates receptor phosphorylation. This way, receptor dimerization and active complex formation (reactions 3 and 4) will not be modulated by free receptors and intermediate complex collision and the binding reaction rate $k'_{on} = k_{on}$. Fig. 1b is a scheme for this hypothesis.

Numerical results corresponding to the receptor dimer hypothesis are presented in Fig. 2b, for direct comparison with the receptor monomer case (Fig. 2a). The model predicts that the receptor dimer model will results in twice the amount of the active complex formation (an average of 23 C_3 complexes at the peak) predicted by the receptor monomer model (C_3 complexes, with a maximum of only 10 molecules at time t = 20 min). This is consistent with the fact that receptor diffusion is slowing down the formation of the complex by modulating the binding rate k_{on}, which in the case of the receptor monomer model is dependent on the amount of available free receptors. Surprisingly, despite the differences in the active complex formation mechanism, both models produce equivalent dynamics of the signaling. This complicates the discrimination between the two hypotheses by direct comparison with current experimental data and more quantitative measurements of absolute values of active complexes are needed to distinguish between the experimental possibilities.

On the other hand, the receptor dimer model seems to be incompatible with the fact that both auto-inhibition and ligand homodimer effect occur in the same system. The only possibility that these two effects can be compatible with experimental data is that each receptor homodimer complex will be able to accommodate two ligands, producing a 2:2 ligand–receptor configuration. This way, two linked ligands in an homodimer configuration have to be able to induce the required conformational change necessary for receptor complex activation. On the contrary, the antagonist effect at high ligand concentrations requires that two non-linked ligands have to fail in bringing the two receptors together and induce activation, creating an auto-inhibitory effect. Other hypotheses for the unstimulated receptor configuration assume a weak interaction between the inter-membrane domains of two free unstimulated receptors [34]. In this situation, the maximum concentration of C_3 will be between the values obtained for the free receptor and the receptor dimer model, depending on the ratio $K_{RR,D}/K_{2,D}$. These three hypotheses are illustrated in Fig. 1c.

Appendix B. Deterministic modeling

When the number of molecules involved is high enough, stochastic integrations may not be necessary and a determinist integration of the model will produce accurate results. Regarding the deterministic approach, the model can be written as 6 ordinary differential equations, one for each of the variables. The equations derived from reactions 1 to 8 can be written as follows:

$$\frac{dR}{dt} = k_{1,off}C_1 + k_{2,off}C_2 - Rk'_{on}(L_2 + L_1) \tag{B.1}$$

$$-2k_{on}RL + 2k_{rec}C_3 + Q_R - k_{R,in}R \tag{B.2}$$

$$\frac{dC_1}{dt} = k_{on}RL - Rk'_{on}L_2 - \left(k_{1,off} + k_{R,in}\right)C_1 + k_{2,off}C_3 \tag{B.3}$$

$$\frac{dC_2}{dt} = k_{on}RL - Rk'_{on}L_1 - \left(k_{2,off} + k_{R,in}\right)C_2 + k_{1,off}C_3 \tag{B.4}$$

$$\frac{dC_3}{dt} = Rk'_{on}(L_1 + L_2) - \left(k_{1,off} + k_{2,off} + k_{3,in}\right)C_3 \tag{B.5}$$

$$\frac{dS}{dt} = k_{3,in}C_3 - \left(k_{S,deg} + k_{rec}\right)S \tag{B.6}$$

$$\frac{dL}{dt} = \frac{k_{1,off}C_1 + k_{2,off}C_2 - 2k_{on}RL + k_{rec}S}{N_{Av}V} \tag{B.7}$$

where all the parameters used above were defined when introducing the stochastic model. The differences between receptor dimer and receptor monomer model are again included in k_{on} in the form of a collision rate constant (see Eq. (12)). Numerical simulations using the equations for the deterministic model (not shown) predict a very different dynamics that the averaged trajectories of the stochastic modeling [42]. This is probably due to the very low number of intermediate complexes C_2 and C_1 formed, so the deterministic approach produces unrealistic predictions in this case, but it will be valid for situations with higher amounts of molecules involved.

References

[1] C.L. Arteaga, The epidermal growth factor receptor: from mutant oncogene in nonhuman cancers to therapeutic target in human neoplasia, J. Clin. Oncol. 19 (18 Suppl) (2001) 32S40S.
[2] J.W. Eschbach, J.C. Egrie, M.R. Downing, J.K. Browne, J.W. Adamson, Correction of the anemia of end-stage renal disease with recombinant human erythropoietin. Results of a combined phase i and ii clinical trial, N. Engl. J. Med. 316 (2) (1987) 738.
[3] M. Fischl, J.E. Galpin, J.D. Levine, J.E. Groopman, D.H. Henry, P. Kennedy, S. Miles, W. Robbins, B. Starrett, R. Zalusky, Recombinant human erythropoietin for patients with aids treated with zidovudine, N. Engl. J. Med. 322 (21) (1990) 148893.
[4] S.N. Constantinescu, X. Liu, W. Beyer, A. Fallon, S. Shekar, Y.I. Henis, S.O. Smith, H.F. Lodish, Activation of the erythropoietin receptor by the gp55-p viral envelope protein is determined by a single amino acid in its transmembrane domain, EMBO J. 18 (12) (1999) 333447.
[5] Griffiths et al, The role of the T lymphocytic cell cycle and an autogenous lymphocytic factor in clinical medicine, Cytobios 93 (372) (1998) 49–66.
[6] P.E. Kovanen, W.J. Leonard, Cytokines and immunodeficiency diseases: critical roles of the gamma(c)-dependent cytokines interleukins 2, 4, 7, 9, 15, and 21, and their signaling pathways, Immunol. Rev. 202 (2004) 6783.
[7] D.A. Laufenburger, J.J. Linderman, Receptors: Models for Binding, Tracking, and Signaling, 1993, p. 376.
[8] H. Shankaran, H. Resat, H. Wiley, Cell surface receptors for signal transduction and ligand transport: a design principles study, PLoS Comput. Biol. 3 (6) (2007) e101.
[9] S.T. Sawyer, S.B. Krantz, E. Goldwasser, Binding and receptor-mediated endocytosis of erythropoietin in friend virus-infected erythroid cells, J. Biol. Chem. 262 (12) (1987) 555462.
[10] S.S. Watowich, H. Wu, M. Socolovsky, U. Klingmuller, S.N. Constantinescu, H.F. Lodish, Cytokine receptor signal transduction and the control of hematopoietic cell development, Annu. Rev. Cell. Dev. Biol. 12 (1996) 91128.
[11] S. Constantinescu, S. Ghaffari, H. Lodish, The erythropoietin receptor: structure, activation and intracellular signal transduction, Trends Endocrinol. Metab. 10 (1) (1999) 18–23.
[12] A. Brooks, J. Wooh, K. Tunny, M. Waters, Growth hormone receptor; mechanism of action, Int. J. Biochem. Cell Biol. 40 (2007) 1984–1989.
[13] J.S. Philo, K.H. Aoki, T. Arakawa, L.O. Narhi, J. Wen, Dimerization of the extracellular domain of the erythropoietin (epo) receptor by epo: one high-affinity and one low-affinity interaction, Biochemistry 35 (5) (1996) 168191.
[14] A.W. Gross, H.F. Lodish, Cellular trafficking and degradation of erythropoietin and novel erythropoiesis stimulating protein (nesp), J. Biol. Chem. 281 (4) (2006) 202432.
[15] S. Elliott, T. Lorenzini, S. Asher, K. Aoki, D. Brankow, L. Buck, L. Busse, D. Chang, J. Fuller, J. Grant, N. Hernday, M. Hokum, S. Hu, A. Knudten, N. Levin, R. Komorowski, F. Martin, R. Navarro, T. Osslund, G. Rogers, N. Rogers, G. Trail, J. Egrie, Enhancement of therapeutic protein in vivo activities through glycoengineering, Nat. Biotechnol. 21 (4) (2003) 41421.
[16] R.S. Syed, S.W. Reid, C. Li, J.C. Cheetham, K.H. Aoki, B. Liu, H. Zhan, T.D. Osslund, A.J. Chirino, J. Zhang, J. Finer-Moore, S. Elliott, K. Sitney, B.A. Katz, Efficiency of signalling through cytokine receptors depends critically on receptor orientation, Nature 395 (1998) 511–516.
[17] A. Yoshimura, A.D. DÕAndrea, H.F. Lodish, Friend spleen focus-forming virus glycoprotein gp55 interacts with the erythropoietin receptor in the endoplasmic reticulum and affects receptor metabolism, Proc. Natl. Acad. Sci. U. S. A. 87 (11) (1990) 413943.
[18] D.J. Hilton, S.S. Watowich, P.J. Murray, H.F. Lodish, Increased cell surface expression and enhanced folding in the endoplasmic reticulum of a mutant erythropoietin receptor, Proc. Natl. Acad. Sci. U. S. A. 92 (1) (1995) 1904.
[19] U. Alon, An introduction to Systems Biology: Design Principles of Biological Circuits, Taylor and Francis Group, FL, USA, 2006.
[20] T. Takahashi, S. Chiba, N. Hirano, Y. Yazaki, H. Hirai, Characterization of three erythropoietin (epo)-binding proteins in various human epo-responsive cell lines and in cells transfected with human epo-receptor cdna, Blood 85 (1) (1995) 10614.

[21] S.T. Sawyer, Introduction: the erythropoietin receptor and signal transduction, Ann. N. Y. Acad. Sci. 718 (1994) 18590.
[22] D. Gillespie, A general method for numerically simulating the stochastic time evolution of coupled chemical reactions, J. Comput. Phys. 2 (1976) 403–434.
[23] D. Gillespie, Exact stochastic simulation of coupled chemical reactions, J. Phys. Chem. 81 (1977) 2340–2361.
[24] D. Gillespie, Stochastic simulation of chemical kinetics, Annu. Rev. Phys. Chem. 58 (2007) 35–55.
[25] H. Qiu, A. Belanger, H.W. Yoon, H.F. Bunn, Homodimerization restores biological activity to an inactive erythropoietin mutant, J. Biol. Chem. 273 (18) (1998) 11173–11176.
[26] J.W. Mockridge, R. Aston, D.J. Morrell, A.T. Holder, Cross-linked growth hormone dimers have enhanced biological activity, Eur. J. Endocrinol. 138 (4) (1998) 44959.
[27] A.J. Sytkowski, E.D. Lunn, K.L. Davis, L. Feldman, S. Siekman, Human erythropoietin dimers with markedly enhanced in vivo activity, Proc. Natl. Acad. Sci. U. S. A. 95 (3) (1998) 11848.
[28] A.J. Sytkowski, E.D. Lunn, M.A. Risinger, K.L. Davis, An erythropoietin fusion protein comprised of identical repeating domains exhibits enhanced biological properties, J. Biol. Chem. 274 (35) (1999) 247738.
[29] H. Schneider, W. Chaovapong, D.J. Matthews, C. Karkaria, R.T. Cass, H. Zhan, M. Boyle, T. Lorenzini, S.G. Elliott, L.B. Giebel, Homodimerization of erythropoietin receptor by a bivalent monoclonal antibody triggers cell proliferation and differentiation of erythroid precursors, Blood 89 (2) (1997) 47382.
[30] G. Fuh, B.C. Cunningham, R. Fukunaga, S. Nagata, D.V. Goeddel, J.A. Wells, Rational design of potent antagonists to the human growth hormone receptor, Science 256 (5064) (1992) 167780.
[31] J.C. Cheetham, D.M. Smith, K.H. Aoki, J.L. Stevenson, T.J. Hoeffel, R.S. Syed, J. Egrie, T.S. Harvey, NMR structure of human erythropoietin and a comparison with its receptor bound conformation, Nat. Struct. Biol. 5 (10) (1998) 861–866.
[32] I.A. Swinburne, D.G. Miguez, D. Landgraf, P.A. Silver, Intron length increases oscillatory periods of gene expression in animal cells, Genes Dev. 22 (17) (2008) 2342–2346.
[33] B.L. Ebert, H.F. Bunn, Regulation of the erythropoietin gene, Blood 94 (6) (1999) 186477.
[34] S.J. Frank, Receptor dimerization in GH and erythropoietin action — it takes two to tango, but how? Endocrinology 143 (1) (2002) 210.
[35] O. Livnah, E.A. Stura, S.A. Middleton, D.L. Johnson, L.K. Jolliffe, I.A. Wilson, Crystallographic evidence for preformed dimers of erythropoietin receptor before ligand activation, Science 283 (5404) (1999) 98790.
[36] I. Remy, I.A. Wilson, S.W. Michnick, Erythropoietin receptor activation by a ligand-induced conformation change, Science 283 (5404) (1999) 9903.
[37] X. Lu, A.W. Gross, H.F. Lodish, Active conformation of the erythropoietin receptor: random and cysteine-scanning mutagenesis of the extracellular juxta-membrane and transmembrane domains, J. Biol. Chem. 281 (11) (2006) 700211.
[38] S.N. Constantinescu, T. Keren, M. Socolovsky, H. Nam, Y.I. Henis, H.F. Lodish, Ligand-independent oligomerization of cell-surface erythropoietin receptor is mediated by the transmembrane domain, Proc. Natl. Acad. Sci. U. S. A. 98 (8) (2001) 437984.
[39] M. Horky, G. Wurzer, V. Kotala, M. Anton, B. Vo jtùesek, J. Vacha, J. Wesierska-Gadek, Segregation of nucleolar components coincides with caspase-3 activation in cisplatin-treated hela cells, J. Cell Sci. 114 (Pt 4) (2001) 66370.
[40] G.M. Hillman, J. Schlessinger, Lateral diffusion of epidermal growth factor complexed to its surface receptors does not account for the thermal sensitivity of patch formation and endocytosis, Biochemistry 21 (7) (1982) 166772.
[41] O. Livnah, E.A. Stura, D.L. Johnson, S.A. Middleton, L.S. Mulcahy, N.C. Wrighton, W.J. Dower, L.K. Jolliffe, I.A. Wilson, Functional mimicry of a protein hormone by a peptide agonist: the epo receptor complex at 2.8 a, Science 273 (5274) (1996) 46471.
[42] Srivastava, et al., Stochastic vs. deterministic modeling of intracellular viral kinetics, J. Theor. Biol. 218 (3) (2002) 309–321.